Journal of the Physical Society of Japan **92**, 054703 (2023)
https://doi.org/10.7566/JPSJ.92.054703

Spin Susceptibility of a $J = 3/2$ Superconductor

Dakyeong Kim[1], Takumi Sato[1], Shingo Kobayashi[2], and Yasuhiro Asano[1]

[1]*Department of Applied Physics, Hokkaido University, Sapporo 060-8628, Japan*
[2]*RIKEN Center for Emergent Matter Science, Wako, Saitama 351-0198, Japan*

(Received February 8, 2023; accepted March 11, 2023; published online April 7, 2023)

We discuss the spin susceptibility of superconductors in which a Cooper pair consists of two electrons having the angular momentum $J = 3/2$ due to strong spin–orbit interactions. The susceptibility is calculated analytically for several pseudospin quintet states within the linear response to a Zeeman field. The susceptibility for A_{1g} symmetry states is isotropic in real space. For E_g and T_{2g} symmetry cases, the susceptibility is anisotropic depending sensitively on choices of order parameter. We also find in T_{2g} states that the susceptibility tensor has off-diagonal elements.

1. Introduction

Spin–orbit interaction is a source of exotic electronic states realized in topological semimetals,[1,2] topological insulators,[3,4] and topological superconductors.[5–9] In the presence of strong spin–orbit interactions, spin $S = 1/2$ and orbital angular momentum $L = 1$ of an electron are inseparable degrees of freedom. Electronic properties of such materials are characterized by an electron with pseudospin $J = L + S = 3/2$. Recent studies have suggested a possibility of superconductivity due to Cooper pairing between two electrons with $J = 3/2$.[10,11] The large angular momentum of an electron enriches the symmetry of the order parameter such as pseudospin-quintet even-parity and pseudospin-septet odd-parity[12–14] in addition to conventional spin-singlet even-parity and spin-triplet odd-parity. Such high angular-momentum pairing states would feature superconducting phenomena of $J = 3/2$ superconductors.[15–23] In particular, a large angular momentum of a Cooper pair would qualitatively change the magnetic response of a superconductor to an external magnetic field.

The spin susceptibility reflects well the internal spin structures of a Cooper pair. It is well known in spin-singlet superconductors that the spin susceptibility decreases monotonically with the decrease of temperature below T_c and vanishes at zero temperature.[24] This phenomenon occurs independently of the direction of a Zeeman field $\boldsymbol{H}$ because a Cooper pair has no spin. In spin-triplet superconductors, on the other hand, the susceptibility can be anisotropic depending on the relative alignment between a Zeeman field and a $\boldsymbol{d}$ vector in the order parameter. For $\boldsymbol{d} \perp \boldsymbol{H}$, the spin susceptibility is constant independent of temperature. Thus, the unchanged Knight shift across T_c in experiments could be strong evidence of spin-triplet superconductivity. For $\boldsymbol{d} \parallel \boldsymbol{H}$, the susceptibility decreases with decreasing temperature below T_c. Such anisotropy is more remarkable when the number of components in a $\boldsymbol{d}$ vector is smaller. For $J = 3/2$ superconductors, however, our knowledge of the spin susceptibility is very limited to a theoretical paper that reported vanishing the spin susceptibility at zero temperature for a singlet-quintet mixed state in a centrosymmetric superconductor.[25]

In this paper, we study theoretically the response of pseudospin-quintet even-parity superconductors to an external Zeeman field. The angular momentum of a Cooper pair in such superconductors is $J = 2$. Since the pairing symmetries of the pseudospin-quintet states are not well understood, we decided to calculate the spin susceptibility for the plausible pair potentials preserving time-reversal symmetry. The spin susceptibility is analytically calculated based on the linear response formula.[26] The pair potential of pseudospin-quintet states is described by a five-component vector that couples to five 4×4 matrices in pseudospin space. Such complicated internal structures of the pair potential enrich the magnetic response of $J = 3/2$ superconductors. For high symmetry pair potentials in pseudospin space (A_{1g} states), the magnetic response is isotropic in real space and the spin susceptibility decreases monotonically with the decrease of temperature. The results are similar to those of ^{3}He B-phase. When the pair potential are independent of wavenumber for lower symmetry states (T_{2g} and E_g), the magnetic response becomes anisotropic in real space. In addition, we find that the susceptibility tensor has finite off-diagonal elements in T_{2g} states.

This paper is organized as follows. In Sect. 2, we explain the tools that describe the electronic structures and the pair potentials of $J = 3/2$ superconductors. In Sect. 3, we discuss the pair potentials considered in this paper and the normal states that stabilize them. The characteristic behaviors of the spin-susceptibility are discussed in Sect. 4. The conclusion is given in Sect. 5. Algebras of 4×4 matrices and a number of mathematical relationships used in the paper are summarized in Appendices. Throughout this paper, we use the system of units $\hbar = k_B = c = 1$, where k_B is the Boltzmann constant and c is the speed of light.

2. $J = 3/2$ Superconductor

We begin our analysis with the normal state Hamiltonian adopted in Ref. 13. The electronic states have four degrees of freedom consisting of two orbitals of equal parity and spin 1/2. In the presence of strong spin–orbit interactions, the effective Hamiltonian for a $J = 3/2$ electron is given by[27,28]

$$\mathcal{H}_N = \sum_{\boldsymbol{k}} \Psi_{\boldsymbol{k}}^{\dagger} H_N(\boldsymbol{k}) \Psi_{\boldsymbol{k}}, \tag{1}$$

$$\Psi_{\boldsymbol{k}} = [c_{\boldsymbol{k},3/2}, c_{\boldsymbol{k},1/2}, c_{\boldsymbol{k},-1/2}, c_{\boldsymbol{k},-3/2}]^{\mathrm{T}}, \tag{2}$$

where T means the transpose of a matrix and $c_{\boldsymbol{k},j_z}$ is the annihilation operator of an electron at $\boldsymbol{k}$ with the z-component of angular momentum being j_z. The normal state Hamiltonian is represented by

$$H_N(\boldsymbol{k}) = \alpha \boldsymbol{k}^2 + \beta(\boldsymbol{k} \cdot \boldsymbol{J})^2 - \mu = \xi_{\boldsymbol{k}} 1_{4\times4} + \vec{\epsilon}_{\boldsymbol{k}} \cdot \vec{\gamma} \tag{3}$$

with $\xi_{\boldsymbol{k}} = \epsilon_{\boldsymbol{k},0} - \mu$ and

$$\epsilon_{k,0} = \left(\alpha + \frac{5}{4}\beta\right)\boldsymbol{k}^2, \quad \epsilon_{k,j} = \beta \boldsymbol{k}^2 e_j c_j(\hat{\boldsymbol{k}}), \tag{4}$$

$$c_1(\hat{\boldsymbol{k}}) = \sqrt{15}\,\hat{k}_x \hat{k}_y, \quad c_2(\hat{\boldsymbol{k}}) = \sqrt{15}\,\hat{k}_y \hat{k}_z, \tag{5}$$

$$c_3(\hat{\boldsymbol{k}}) = \sqrt{15}\,\hat{k}_z \hat{k}_x, \quad c_4(\hat{\boldsymbol{k}}) = \frac{\sqrt{15}}{2}(\hat{k}_x^2 - \hat{k}_y^2), \tag{6}$$

$$c_5(\hat{\boldsymbol{k}}) = \frac{\sqrt{5}}{2}(2\hat{k}_z^2 - \hat{k}_x^2 - \hat{k}_y^2), \tag{7}$$

where $\hat{k}_j = k_j/|\boldsymbol{k}|$ for $j = x$, y, and z represents the direction of wavenumber on the Fermi surface. The constants $\alpha > 0$ and β determine the normal state property. The spin–orbit interactions increase with the increase of $\beta > 0$. The coefficients c_j are normalized as

$$\langle c_i(\hat{\boldsymbol{k}})c_j(\hat{\boldsymbol{k}})\rangle_{\hat{k}} \equiv \int \frac{d\hat{\boldsymbol{k}}}{4\pi} c_i(\hat{\boldsymbol{k}})c_j(\hat{\boldsymbol{k}}) = \delta_{i,j}, \tag{8}$$

where $\langle\cdots\rangle_{\hat{k}}$ means the integral over the solid angle on the Fermi surface. The normalized five-component vector $\vec{e} = (e_1, e_2, e_3, e_4, e_5)/|\vec{e}|$ determines the dependence of the normal state dispersions on pseudospins. The spinors for the angular momentum of $J = 3/2$ are described by,

$$J_x = \frac{1}{2}\begin{bmatrix} 0 & \sqrt{3} & 0 & 0 \\ \sqrt{3} & 0 & 2 & 0 \\ 0 & 2 & 0 & \sqrt{3} \\ 0 & 0 & \sqrt{3} & 0 \end{bmatrix}, \tag{9}$$

$$J_y = \frac{1}{2}\begin{bmatrix} 0 & -i\sqrt{3} & 0 & 0 \\ i\sqrt{3} & 0 & -2i & 0 \\ 0 & 2i & 0 & -i\sqrt{3} \\ 0 & 0 & i\sqrt{3} & 0 \end{bmatrix}, \tag{10}$$

$$J_z = \frac{1}{2}\begin{bmatrix} 3 & 0 & 0 & 0 \\ 0 & 1 & 0 & 0 \\ 0 & 0 & -1 & 0 \\ 0 & 0 & 0 & -3 \end{bmatrix}. \tag{11}$$

The 4×4 matrices in pseudospin space are defined as

$$\gamma^1 = \frac{1}{\sqrt{3}}(J_x J_y + J_y J_x), \quad \gamma^2 = \frac{1}{\sqrt{3}}(J_y J_z + J_z J_y), \tag{12}$$

$$\gamma^3 = \frac{1}{\sqrt{3}}(J_z J_x + J_x J_z), \quad \gamma^4 = \frac{1}{\sqrt{3}}(J_x^2 - J_y^2), \tag{13}$$

$$\gamma^5 = \frac{1}{3}(2J_z^2 - J_x^2 - J_y^2), \tag{14}$$

and $1_{4\times4}$ is the identity matrix. They satisfy the following relations

$$\gamma^\nu \gamma^\lambda + \gamma^\lambda \gamma^\nu = 2 \times 1_{4\times4}\delta_{\nu,\lambda}, \tag{15}$$

$$\gamma^1 \gamma^2 \gamma^3 \gamma^4 \gamma^5 = -1_{4\times4}, \tag{16}$$

$$\{\gamma^\nu\}^* = \{\gamma^\nu\}^{\mathrm{T}} = U_T \gamma^\nu U_T^{-1}, \quad U_T = \gamma^1 \gamma^2, \tag{17}$$

where U_T is the unitary part of the time-reversal operation $\mathcal{T} = U_T \mathcal{K}$ with $\mathcal{K}$ meaning complex conjugation. The superconducting pair potential is represented as

$$\Delta(\boldsymbol{k}) = \vec{\eta}_{\boldsymbol{k}} \cdot \vec{\gamma}\, U_T, \tag{18}$$

where a five-component vector $\vec{\eta}_{\boldsymbol{k}}$ represents an even-parity pseudospin-quintet state. Throughout this paper, we assume that all components of $\vec{\eta}_{\boldsymbol{k}}$ are real values. As a result of the Fermi–Dirac statistics of electrons, the pair potential is antisymmetric under the permutation of two pseudospins, [i.e., $\Delta^{\mathrm{T}}(\boldsymbol{k}) = -\Delta(\boldsymbol{k})$]. The Bogoliubov–de Gennes Hamiltonian reads,

$$H_{\mathrm{BdG}}(\boldsymbol{k}) = \begin{bmatrix} H_{\mathrm{N}}(\boldsymbol{k}) & \Delta(\boldsymbol{k}) \\ -\underset{\sim}{\Delta}(\boldsymbol{k}) & -\underset{\sim}{H}_{\mathrm{N}}(\boldsymbol{k}) \end{bmatrix}, \tag{19}$$

where $\underset{\sim}{X}(\boldsymbol{k}, i\omega) \equiv X^*(-\boldsymbol{k}, i\omega)$ represents the particle–hole conjugation of $X(\boldsymbol{k}, i\omega)$.

The interaction with a uniform Zeeman field $\boldsymbol{H}$ is described by[27]

$$H_{\mathrm{Z}} = -\mu_{\mathrm{B}} \tilde{\boldsymbol{J}} \cdot \boldsymbol{H}, \tag{20}$$

$$\tilde{J}_j = g_1 J_j + g_3 J_j^3, \tag{21}$$

for $j = x$, y, and z, where μ_{B} is the Bohr's magneton, and g_1 and g_3 are the coupling constants. The matrix structures of J_j and J_j^3 are displayed in Appendix A. The angular momenta in the Zeeman Hamiltonian are then given by

$$\tilde{J}_x = -\frac{i}{2}(\sqrt{3}p_1\gamma^2\gamma^5 + p_2\gamma^1\gamma^3 + p_1\gamma^2\gamma^4), \tag{22}$$

$$\tilde{J}_y = \frac{i}{2}(\sqrt{3}p_1\gamma^3\gamma^5 + p_2\gamma^1\gamma^2 - p_1\gamma^3\gamma^4), \tag{23}$$

$$\tilde{J}_z = \frac{i}{2}(p_2\gamma^2\gamma^3 + 2p_1\gamma^1\gamma^4), \tag{24}$$

$$p_1 = g_1 + \frac{7}{4}g_3, \quad p_2 = g_1 + \frac{13}{4}g_3. \tag{25}$$

In the linear response theory, the spin susceptibility is calculated by using the formula[26]

$$\begin{aligned} \chi_{\mu\nu} = \chi_{\mathrm{N}}\,\delta_{\mu,\nu} - \left(\frac{\mu_{\mathrm{B}}}{2}\right)^2 T \sum_{\omega_n} \int \frac{d\boldsymbol{k}}{(2\pi)^3} \\ \times \mathrm{Tr}[G(\boldsymbol{k}, i\omega_n)\,\tilde{J}_\mu\, G(\boldsymbol{k}, i\omega_n)\,\tilde{J}_\nu \\ + \underset{\sim}{F}(\boldsymbol{k}, i\omega_l)\,\tilde{J}_\mu\, F(\boldsymbol{k}, i\omega_n)(\tilde{J}_\nu)^* \\ - G_{\mathrm{N}}(\boldsymbol{k}, i\omega_n)\,\tilde{J}_\mu\, G_{\mathrm{N}}(\boldsymbol{k}, i\omega_n)\,\tilde{J}_\nu]. \end{aligned} \tag{26}$$

The summation over the Matsubara frequency and that over the wavenumber are regularized by introducing the Green's functions in the normal state G_{N} and the spin susceptibility χ_{N} in the normal state.[29]

The Green's function for a superconducting state can be obtained by solving the Gor'kov equation

$$\begin{aligned} [i\omega_n - H_{\mathrm{BdG}}(\boldsymbol{k})]\begin{bmatrix} G(\boldsymbol{k}, i\omega_n) & F(\boldsymbol{k}, i\omega_n) \\ -\underset{\sim}{F}(\boldsymbol{k}, i\omega_n) & -\underset{\sim}{G}(\boldsymbol{k}, i\omega_n) \end{bmatrix} \\ = 1_{8\times8}. \end{aligned} \tag{27}$$

The anomalous Green's function results in

$$\begin{aligned} F^{-1}(\boldsymbol{k}, i\omega_n) = \frac{U_T}{\vec{\eta}_{\boldsymbol{k}}{}^2}[(\omega_n^2 + \xi_{\boldsymbol{k}}{}^2 + \vec{\eta}_{\boldsymbol{k}}{}^2)\vec{\eta}_{\boldsymbol{k}} \cdot \vec{\gamma} \\ + i\omega_n[\vec{\eta}_{\boldsymbol{k}} \cdot \vec{\gamma}, \vec{\epsilon}_{\boldsymbol{k}} \cdot \vec{\gamma}]_- \\ + 2\xi_{\boldsymbol{k}}\,\vec{\eta}_{\boldsymbol{k}} \cdot \vec{\epsilon}_{\boldsymbol{k}} + (\vec{\epsilon}_{\boldsymbol{k}} \cdot \vec{\gamma})(\vec{\eta}_{\boldsymbol{k}} \cdot \vec{\gamma})(\vec{\epsilon}_{\boldsymbol{k}} \cdot \vec{\gamma})]. \end{aligned} \tag{28}$$

Generally speaking, it is not easy to calculate analytically the inversion of 4×4 matrices.

3. Choice of Pair Potentials and Normal States

The original normal state Hamiltonian in Eq. (3) is spheric in both momentum and pseudospin spaces. For a cubic symmetric superconductor,[15] in which even-parity pair potentials are classified into A_{1g}, E_g, and T_{2g} states according to irreducible representations (irreps) of cubic symmetry. With focusing on pseudospin-quintet Cooper pairs, their pairing states are explicitly represented as

$$A_{1g}:\quad \vec{\eta}_{\boldsymbol{k}} \cdot \vec{\gamma} = \Delta \sum_{j=1}^{5} h_j\, c_j(\hat{\boldsymbol{k}})\, \gamma^j, \tag{29}$$

$$E_g:\quad \vec{\eta}_{\boldsymbol{k}} \cdot \vec{\gamma} = \Delta(l_4\gamma^4 + l_5\gamma^5), \tag{30}$$

$$T_{2g}:\quad \vec{\eta}_{\boldsymbol{k}} \cdot \vec{\gamma} = \Delta(l_1\gamma^1 + l_2\gamma^2 + l_3\gamma^3), \tag{31}$$

where the unit vector $\vec{h}$ determines the pseudospin structure of A_{1g} state and $l_i \in \mathbb{C}$ $(i = 1\text{–}5)$. A_{1g} states involve momentum-dependent coefficients, which comes from the fact that γ^4 and γ^5 (γ^1, γ^2, and γ^3) themselves belong to E_g (T_{2g}) irreps of cubic symmetry.

Generally speaking, the coefficients l_i for $i = 1\text{–}5$ are determined from the steady states of the free energy.[30] For E_g state, three distinct steady states exist: $(l_4, l_5) = (1, 0)$, $(0, 1)$, and $(1, i)/\sqrt{2}$. The first two states preserve time-reversal symmetry, while the last state breaks time-reversal symmetry. For T_{2g} state, there are four distinct steady states: $(l_1, l_2, l_3) = (1, 1, 1)/\sqrt{3}$, $(1, 0, 0)$, $(1, e^{i2\pi/3}, e^{i4\pi/3})/\sqrt{3}$, $(1, i, 0)/\sqrt{2}$. The last two states break time-reversal symmetry. Time-reversal symmetry-breaking superconducting states have a problem specific to them: the formation of Bogoliubov–Fermi surfaces.[13,15,20] Since the relations between the pseudospin structures of a Cooper pair and the magnetic response of a superconductor is the main issue in this paper, we focus on time-reversal symmetry respecting superconducting states. In addition to the steady states, we also consider another pseudospin states described by $(l_4, l_5) = (1, 1)/\sqrt{2}$, $(l_1, l_2, l_3) = (1, 1, 0)/\sqrt{2}$, and $(l_1, l_2, l_3, l_4, l_5) = (1, 1, 1, 1, 1)/\sqrt{5}$. The last one is the admixture of E_g and T_{2g} states. These states complement possible combinations of γ^i $(i = 1\text{–}5)$. The comparison between the calculated results for such states and those for the steady states helps us to understand the relations between the pseudospin structures of a Cooper pair and the spin susceptibility.

As shown in the second term in Eq. (28), the anomalous Green's function contains the pairing correlation belonging to odd-frequency symmetry class. The stable superconducting states can be described by

$$A_{\rm odd} = [\vec{\eta}_{\boldsymbol{k}} \cdot \vec{\gamma}, \vec{\epsilon}_{\boldsymbol{k}} \cdot \vec{\gamma}]_- = 0, \tag{32}$$

which means the absence of odd-frequency pairs. Odd-frequency pairs increase the free-energy of a uniform superconducting state[31] because they indicate the paramagnetic response to a magnetic field.[32–34] A phenomenological argument on the paramagnetic response of odd-frequency Cooper pairs is given in Appendix A of Ref. 35. Equation (32) gives a guide that relates the stable pair potential $\vec{\eta}$ to the electronic structures $\vec{\epsilon}$.

To make the meaning of Eq. (32) clear, we discuss two practical cases. First we briefly summarize the case of spin-triplet superconductors in the presence of a strong Rashba spin–orbit interaction $\boldsymbol{\lambda} \cdot \boldsymbol{\sigma}$ with

$$\boldsymbol{\lambda} = \lambda_{\rm so}(\hat{k}_y \boldsymbol{e}_x - \hat{k}_x \boldsymbol{e}_y), \tag{33}$$

where $\lambda_{\rm so}$ represents the amplitude of spin–orbit interaction, σ_j and $\boldsymbol{e}_j$ for $j = x$, y, and z are the Pauli matrix and the unit vector in spin space, respectively. The stable order parameter $i\boldsymbol{d} \cdot \boldsymbol{\sigma}\sigma_y$ is determined as

$$[\boldsymbol{d} \cdot \boldsymbol{\sigma}, \boldsymbol{\lambda} \cdot \boldsymbol{\sigma}]_- = 0 \quad \text{or} \quad \boldsymbol{d} \parallel \boldsymbol{\lambda}, \tag{34}$$

so that odd-frequency pairs are absent and the transition temperature is optimal.[31,36] Namely, the order parameter of a spin helical state is stable in this case. The pair potentials other than the helical state would be realized when the Rashba spin–orbit interaction is sufficiently weak. The choice in Eq. (34) and that in Eq. (32) are equivalent to each other. Secondly we summarize instability of an E_g state with $(l_4, l_5) = (1, i)/\sqrt{2}$ under $\vec{\epsilon} = (1, 1, 1, 1, 1)/\sqrt{5}$. In this case, Eq. (32) is not satisfied. Although such a time-reversal breaking superconducting state takes the minimum of the Ginzburg–Landau free-energy,[12] its phase diagram is very complicated.[37] In some cases, the transition from the normal state to the superconducting state become the first order, which implies the instability of the superconducting state. A paper showed that a term proportional to $\mathrm{Tr}[A_{\rm odd}^2]$ enters the free-energy, increases the free-energy and decreases $T_{\rm c}$.[38] Their conclusion agrees with that of suppression of $T_{\rm c}$ due to odd-frequency Cooper pairs.[31]

In this paper, we choose the normal state dispersion $\vec{\epsilon}_{\boldsymbol{k}}$ so that Eq. (32) is satisfied for the pair potentials in Eqs. (29)–(31). The Green's function in the superconducting state can be expressed simply and analytically under Eq. (32). The results of the Green's function in such a case are shown in Appendix B. As we displayed in Appendix C, the gap equation for the superconducting states satisfying Eq. (32) is identical to that in the BCS theory. The transition to such superconducting states from the normal one is always the second order.

4. Spin Susceptibility

The spin susceptibility for pseudospin-quintet states are calculated as

$$\frac{\chi_{\mu\nu}}{\chi_{\rm N}} = \delta_{\mu,\nu} - \pi T \sum_{\omega_n} \left\langle \frac{1}{2\Omega^3}\left(\vec{\eta}^{\,2}\, \delta_{\mu,\nu} + \frac{L_{\mu,\nu}(\vec{\eta})}{P_+}\right)\right\rangle_{\hat{\boldsymbol{k}}}, \tag{35}$$

with $\Omega = \sqrt{\omega_n^2 + \vec{\eta}^{\,2}}$. The tensor is defined by

$$L_{\mu,\nu}(\vec{\eta}) \equiv \mathrm{Tr}[\vec{\eta} \cdot \vec{\gamma} \tilde{J}_\mu \vec{\eta} \cdot \vec{\gamma} \tilde{J}_\nu], \tag{36}$$

and its elements are calculated to be

$$L_{xx} = P_-(\eta_1^2 - \eta_2^2 + \eta_3^2) + R_+\eta_4^2 - R_-\eta_5^2 - 4\sqrt{3}p_1^2\,\eta_4\,\eta_5, \tag{37}$$

$$L_{yy} = P_-(\eta_1^2 + \eta_2^2 - \eta_3^2) + R_+\eta_4^2 - R_-\eta_5^2 + 4\sqrt{3}p_1^2\,\eta_4\,\eta_5, \tag{38}$$

$$L_{zz} = P_-(-\eta_1^2 + \eta_2^2 + \eta_3^2 - \eta_4^2) + P_+\eta_5^2, \tag{39}$$

$$L_{xy} = 2\big[P_+\,\eta_2\,\eta_3 - 2\sqrt{3}p_1p_2\eta_1\,\eta_5\big], \tag{40}$$

$$L_{yz} = 2\big[P_+\,\eta_1\,\eta_3 + \sqrt{3}p_1p_2\big(\eta_2\,\eta_5 - \sqrt{3}\eta_2\eta_4\big)\big], \tag{41}$$

$$L_{zx} = 2\big[P_+\,\eta_1\,\eta_2 + \sqrt{3}p_1\,p_2\big(\eta_3\,\eta_5 + \sqrt{3}\eta_3\eta_4\big)\big], \tag{42}$$

$$P_\pm \equiv 4p_1^2 \pm p_2^2, \qquad R_\pm = 2p_1^2 \pm p_2^2. \tag{43}$$

The results in Eqs. (37)–(42) describe the characteristic features of the susceptibility of $J = 3/2$ superconductors.

4.1 A_{1g} state

In the presence of attractive interactions in an A_{1g} channel, the pair potential is represented by Eqs. (18) and (29). We always set $\vec{e} = \vec{h}$ so that Eq. (32) is satisfied. Different from the *s*-wave spin-singlet pairing that also belongs to the A_{1g} irrep, an A_{1g} state in the pseudo-spin quintet pairing has the pseudospin degrees of freedom, which allows us to choose a variety of pseudospin structures. We first choose a pseudospin structure of a T_{2g} irrep characterized by $\vec{h} = \vec{h}_{T_{2g}} = (1, 1, 1, 0, 0)/\sqrt{3}$. The spin susceptibility is calculated as

$$\chi_{\mu\nu} = \chi_{\mathrm{N}}\, \delta_{\mu,\nu}\left[1 - \frac{1}{2}\left(1 + \frac{P_-}{3P_+}\right)\mathcal{Q}\right], \tag{44}$$

$$\mathcal{Q}(T) = \pi T \sum_{\omega_n} \frac{\Delta^2}{\Omega^3}. \tag{45}$$

In BCS theory, $\mathcal{Q}$ represents the fraction of Cooper pairs to quasiparticles on the Fermi surface. Indeed $\mathcal{Q}$ is zero at $T = T_c$, increases monotonically with the decrease of T, and becomes unity at $T = 0$. The susceptibility tensor is diagonal and isotropic in real space. The susceptibility for a pseudospin structure of an E_g irrep characterized by $\vec{h} = \vec{h}_{E_g} = (0, 0, 0, 1, 1)/\sqrt{2}$ results in,

$$\chi_{\mu\nu} = \chi_{\mathrm{N}}\, \delta_{\mu,\nu}\left[1 - \frac{1}{2}\left(1 + \frac{p_2^2}{P_+}\right)\mathcal{Q}\right]. \tag{46}$$

The susceptibility for an admixture of T_{2g} and E_g irreps $[\vec{h}_{T_{2g}+E_g} = (1, 1, 1, 1, 1)/\sqrt{5}]$ is also calculated as

$$\chi_{\mu\nu} = \chi_{\mathrm{N}}\, \delta_{\mu,\nu}\left[1 - \frac{1}{2}\left(1 + \frac{1}{5}\right)\mathcal{Q}\right]. \tag{47}$$

The off-diagonal elements in the susceptibility tensor are always zero in these cases, (i.e., $\chi_{\mu\nu} = 0$ for $\mu \neq \nu$). The pair potentials in these states are represented by

$$\Delta_{T_{2g}} \propto \hat{k}_x \hat{k}_y (J_x J_y + J_y J_x) + \hat{k}_y \hat{k}_z (J_y J_z + J_z J_y) + \hat{k}_z \hat{k}_x (J_z J_x + J_x J_z), \tag{48}$$

$$\Delta_{E_g} \propto \hat{k}_x^2 J_x^2 + \hat{k}_y^2 J_y^2 + \hat{k}_z^2 J_z^2 - \frac{5}{4}. \tag{49}$$

In Fig. 1(a), we plot the susceptibility at $g_3 = 0$ as a function of temperature. The dependence of the pair potential on temperature is calculated by solving the gap equation in the weak coupling limit. As shown in Appendix C, the gap equation is common for all the superconducting states considered in the present paper and is identical to that in BCS theory. The results show that the susceptibility decreases with the decrease of temperature below T_c. The results are independent of such choices of the pseudospin structures as T_{2g}, E_g, and $T_{2g} + E_g$ at $g_3 = 0$. Although a Cooper pair has the angular momentum of $J = 2$ in the quintet states, the susceptibility is isotropic for all the pseudospin structures. The characteristic behaviors are independent of the strength of spin–orbit interaction β/α. The isotropic feature of the spin susceptibility is considered as a result of high symmetry of the pair potential. The pair potentials for a T_{2g} and an E_g irreps shown in Eqs. (48) and (49) are symmetric under the cyclic permutation among x, y, and z. For comparison, we briefly mention the spin susceptibility in superfluid ^{3}He B-phase described by

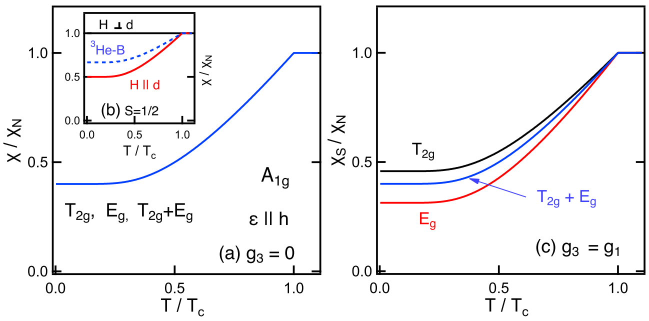

Fig. 1. (Color online) The spin susceptibility for A_{1g} states in the pseudospin-quintet superconductors is plotted as a function of temperature in (a), where we consider $g_3 = 0$ and $\vec{\epsilon} = \vec{h}$. The diagonal elements in the spin susceptibility tensor are isotropic in real space and the off-diagonal elements are zero. In (b), the susceptibility of spin-triplet superconductors are shown for a helical spin-triplet superconductor with two solid lines and for a ^{3}He B-phase with a broken line. In (c), we consider the effects of J_j^3 terms in the Zeeman Hamiltonian by choosing $g_3 = g_1$. Although the amplitudes of susceptibility deviate slightly from those in (a), the characteristic features of the susceptibility retain.

$$\boldsymbol{d} = \Delta(\hat{k}_x \boldsymbol{e}_x + \hat{k}_y \boldsymbol{e}_y + \hat{k}_z \boldsymbol{e}_z). \tag{50}$$

The pair potential is symmetric under the cyclic permutation among x, y, and z. As a result, the susceptibility plotted with a broken line in Fig. 1(b) is isotropic in real space.

At the end of the subsection, we briefly discuss the effects of J_μ^3 term on the spin susceptibility by choosing $g_3 = g_1$. The results are shown in Fig. 1(c). The isotropic nature of the susceptibility remains unchanged even for $g_3 = g_1$. The amplitude of the susceptibility depends on the pseudospin structure of the pair potential; the amplitude for a T_{2g} irrep becomes slightly larger than that for an E_g irrep.

4.2 T_{2g} state

When attractive interactions between two electrons work in a T_{2g} or an E_g channel, the order parameters in Eqs. (30) and (31) are isotropic in momentum space. To satisfy Eq. (32), we switch off $\vec{\epsilon} = 0$ and consider a simple pseudospin quintet superconductor in the following subsections. In other words, the superconducting states characterized by Eqs. (30) and (31) are stable when $|\vec{\epsilon}|$ is sufficiently smaller than the amplitude of the pair potential at $T = 0$. Even if we choose $\vec{\epsilon} = 0$, superconductors show the rich magnetic response depending on the pseudospin structures of the pair potential. The effects of the pseudospin-dependent dispersions $\vec{\epsilon} \neq 0$ on the magnetic response will be discussed later. The pair potential considered in this subsection are represented by

$$\Delta_{T_{2g}(a)} \propto (J_x J_y + J_y J_x) + (J_y J_z + J_z J_y) + (J_z J_x + J_x J_z), \tag{51}$$

$$\Delta_{T_{2g}(b)} \propto (J_x J_y + J_y J_x) + (J_y J_z + J_z J_y), \tag{52}$$

$$\Delta_{T_{2g}(c)} \propto (J_x J_y + J_y J_x). \tag{53}$$

We first discuss a T_{2g} state with $(l_1, l_2, l_3) = (1, 1, 1)/\sqrt{3}$. The pair potential is given by Eq. (51). The diagonal elements shown in Eq. (44) are isotropic because the pair potential is symmetric under the cyclic permutation among x, y, and z. In addition to the diagonal elements, the susceptibility has the off-diagonal elements as

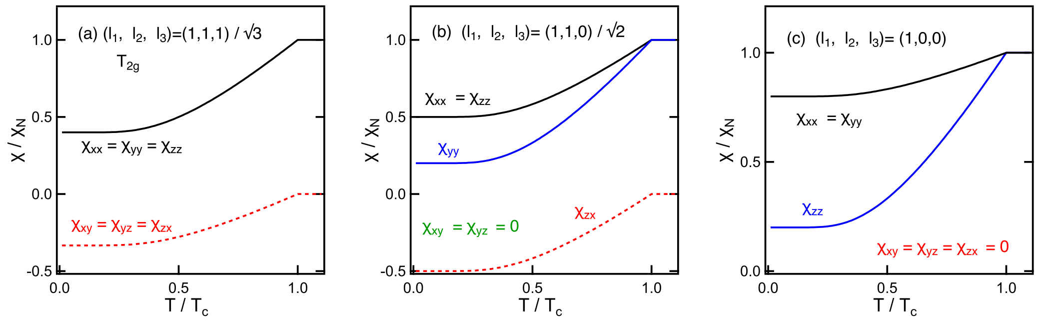

Fig. 2. (Color online) The spin susceptibility is plotted as a function of temperature for a T_{2g} state with $(l_1, l_2, l_3) = (1, 1, 1)/\sqrt{3}$ in (a). The susceptibility tensor in a T_{2g} state has off-diagonal elements. In (b), the results for the state with $(1, 1, 0)/\sqrt{2}$ are displayed, where we delete γ^3 component from the T_{2g} pair potential. The results for a single component pair potential with $(1, 0, 0)/\sqrt{2}$ are shown in (c). Although we put $g_3 = 0$ in these figures, J_j^3 terms in the Zeeman potential do not change the characteristic features.

$$\chi_{xy} = \chi_{yz} = \chi_{zx} = -\chi_{\mathrm{N}} \frac{1}{3} \mathcal{Q}. \tag{54}$$

The results for $g_3 = 0$ are displayed in Fig. 2(a). The pair potential in Eq. (51) includes the off-diagonal terms. As a result, the first term of $L_{\mu\nu}(\vec{\eta})$ in Eqs. (40)–(42) becomes finite. Since the pair potential is independent of wavenumber, these off-diagonal terms remain nonzero values even after averaging over directions in momentum space on the Fermi surface. Thus, the appearance of the off-diagonal elements in the susceptibility tensor is a characteristic feature of a T_{2g} state.

Secondly, we display the susceptibility for a T_{2g} state with $(l_1, l_2, l_3) = (1, 1, 0)/\sqrt{2}$ in Fig. 2(b). The pair potential shown in Eq. (52) is symmetric under the permmutation of J_x and J_z, whereas J_y is no longer equivalent to J_x and J_z. The anisotropy of the diagonal elements in Fig. 2(b) is a direct result of a pair potential at a low symmetry. As shown in Eqs. (40)–(42), the off-diagonal elements are finite only for the multi-component pair potentials. At the present case, only the χ_{zx} element remains finite because of $l_3 = 0$.

Finally, we display the susceptibility for a T_{2g} state with $(l_1, l_2, l_3) = (1, 0, 0)/\sqrt{2}$ in Fig. 2(c). The pair potential in Eq. (53) is symmetric under the exchange between J_x and J_y. The z axis is the high symmetry axis in this case. As a result, the diagonal elements are anisotropic as shown in Fig. 2(c). All the off-diagonal elements vanish because the pair potential has only one pseudospin component.

4.3 E_g state

The pair potential for an E_g state with $(l_4, l_5) = (1, 1)/\sqrt{2}$ becomes

$$\Delta_{E_g(a)} \propto (\sqrt{3} - 1)J_x^2 - (\sqrt{3} + 1)J_y^2 + 2J_z^2, \tag{55}$$

and the susceptibility is calculated as

$$\chi_{xx} = \chi_{\mathrm{N}}\left[1 - \frac{1}{2}\left(1 + \frac{p_2^2 - \sqrt{3}p_1^2}{P_+}\right)\mathcal{Q}\right], \tag{56}$$

$$\chi_{yy} = \chi_{\mathrm{N}}\left[1 - \frac{1}{2}\left(1 + \frac{p_2^2 + \sqrt{3}p_1^2}{P_+}\right)\mathcal{Q}\right], \tag{57}$$

$$\chi_{zz} = \chi_{\mathrm{N}}\left[1 - \frac{1}{2}\left(1 + \frac{p_2^2}{P_+}\right)\mathcal{Q}\right], \tag{58}$$

$$\chi_{xy} = \chi_{yz} = \chi_{zx} = 0. \tag{59}$$

The results are shown in Fig. 3(a). Since J_x, J_y, and J_z are not equivalent to one another in Eq. (55) any longer, the susceptibility becomes anisotropic in three directions. The off-diagonal elements are absent in the susceptibility tensor because the pair potential in Eq. (55) does not include such off-diagonal terms as $J_\mu J_\nu$ with $\mu \neq \nu$.

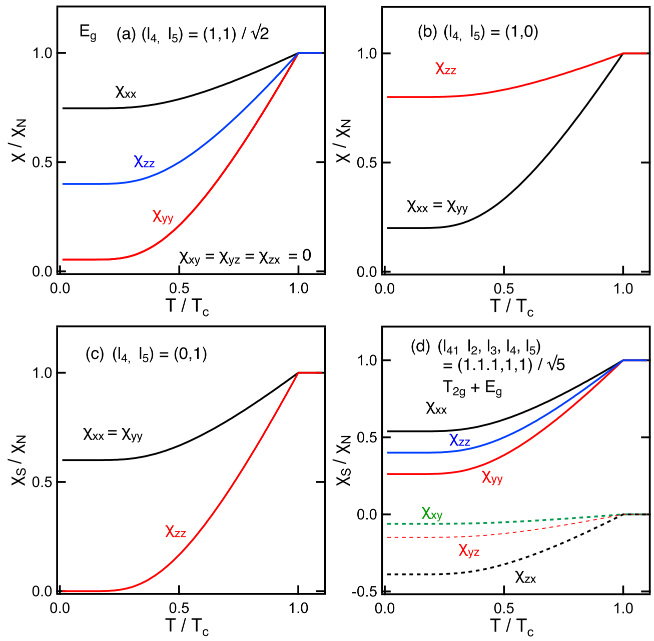

Fig. 3. (Color online) The spin susceptibility is plotted as a function of temperature for a E_g state in (a).

In Figs. 3(b) and 3(c), we display the results for the single component states with $(l_4, l_5) = (1, 0)$ and $(0, 1)$, respectively. They are possible order parameters of E_g states in the presence of time-reversal symmetry.[30] We find the relation

$$\chi_{xx} = \chi_{yy} \neq \chi_{zz}. \tag{60}$$

Their pair potentials $\gamma^4 \propto J_x^2 - J_y^2$ and $\gamma^5 \propto 2J_z^2 - J_x^2 - J_y^2$ remain unchanged under the permmutation of J_x and J_y. Including the results in Fig. 2(c), Eqs. (37)–(42) suggest that the anisotropic response like Eq. (60) and the absence of off-diagonal elements are the common feature of the single component order parameter.

The degree of the anisotropy of the diagonal response in pseudospin-quintet states is rather weaker than that in a spin-triplet superconductor. For comparison, in Fig. 1(b), we plot the susceptibility of a spin-triplet helical state characterized by $\boldsymbol{d} \parallel \boldsymbol{\lambda}$ in Eq. (33) with two solid lines. When a Zeeman field is perpendicular to $\boldsymbol{d}$, the susceptibility is a constant across T_c. The results for $\boldsymbol{H} \parallel \boldsymbol{d}$, on the other hand, the susceptibility decreases down to $(1/2)\chi_N$. These behaviors are independent of the amplitudes of $\lambda_{so} > 0$. In spin-triplet superconductors, both the dimension in spin space and that in real space are three. Therefore, it is possible to define two different directions relatively to the direction of a Zeeman field: ($\boldsymbol{d} \parallel \boldsymbol{H}$ and $\boldsymbol{d} \perp \boldsymbol{H}$). The clear anisotropy of the susceptibility in Fig. 1(b) is a result of the dimensional consistency between in spin space and in real space. The results in Figs. 2 and 3 indicate that the anisotropy of the diagonal elements is more remarkable for the number of components in the pair potential smaller.

4.4 *Admixture of T_{2g} and E_g states*

The results for a the admixture of T_{2g} and E_g states, [i.e., $(l_1, l_2, l_3, l_4, l_5) = (1, 1, 1, 1, 1)/\sqrt{5}$], are calculated as

$$\chi_{xx} = \chi_N\left[1 - \frac{1}{2}\left(1 + \frac{P_+ - 4\sqrt{3}p_1^2}{5P_+}\right)\mathcal{Q}\right], \tag{61}$$

$$\chi_{yy} = \chi_N\left[1 - \frac{1}{2}\left(1 + \frac{P_+ + 4\sqrt{3}p_1^2}{5P_+}\right)\mathcal{Q}\right], \tag{62}$$

$$\chi_{zz} = \chi_N\left[1 - \frac{1}{2}\left(1 + \frac{1}{5}\right)\mathcal{Q}\right]. \tag{63}$$

The off-diagonal elements are calculated in the similar way,

$$\chi_{xy} = -\chi_N\,\mathcal{Q}\,\frac{P_+ - 2\sqrt{3}p_1 p_2}{5P_+}, \tag{64}$$

$$\chi_{yz} = -\chi_N\mathcal{Q}\,\frac{P_+ + \sqrt{3}p_1 p_2(1 - \sqrt{3})}{5P_+}, \tag{65}$$

$$\chi_{zx} = -\chi_N\mathcal{Q}\,\frac{P_+ + \sqrt{3}p_1 p_2(1 + \sqrt{3})}{5P_+}. \tag{66}$$

The calculated results for $g_3 = 0$ are plotted in Fig. 3(d). Not only the diagonal elements but also the off-diagonal elements are anisotropic. All the elements in Eqs. (37)–(42) are finite and different from one another. The degree of the anisotropy in the diagonal elements are weaker than that in E_g state and stronger than that in T_{2g} state. The characteristic features of the susceptibility displayed in Figs. 2 and 3 retain even if we consider J_μ^3 term in the Zeeman Hamiltonian.

Finally, we briefly discuss the effects of the pseudospin-dependent dispersion $\vec{\epsilon}$ on the characteristic behaviors of the susceptibility. When we switch on $\vec{\epsilon}$ in T_{2g} and E_g states, Eq. (32) is no longer holds. As a result, the additional terms such as

$$\frac{C_f}{2}\, i\omega_n[\vec{\eta}_{\boldsymbol{k}} \cdot \vec{\gamma}, \vec{\epsilon}_{\boldsymbol{k}} \cdot \vec{\gamma}]_- = C_f\, i\omega_n \sum_{i\neq j} \epsilon_i\, \eta_j\, \gamma^i\, \gamma^j, \tag{67}$$

appear at the numerator of the anomalous Green's function in Eq. (B·4), where C_f is a constant. Such components represent the admixture of pseudospin-triplet and the pseudospin-septet pairing correlations.[20] Their contribution to the susceptibility tensor is proportional to

$$C_f^2\, \omega_n^2\, \mathrm{Tr}\left[\sum_{i\neq j} \epsilon_i\, \eta_j \gamma^i \gamma^j\, \tilde{J}_\mu \sum_{k\neq l} \epsilon_k\, \eta_l \gamma^k \gamma^l\, \tilde{J}_\nu\right], \tag{68}$$

which modify the susceptibility tensor. However, they do not always cancel the off-diagonal elements in Fig. 2(a) in a T_{2g} state. They do not wash out the anisotropy of the diagonal elements in Fig. 3 in E_g states.

The results in Figs. 1–3 suggest that the behaviors of the susceptibility depends sensitively on the orbital symmetry and the pseudospin structures of the pair potential. In particular, the appearance of the off-diagonal elements in the susceptibility tensor is a characteristic feature of $J = 3/2$ superconductors.

5. Conclusion

We have studied theoretically the spin susceptibility of pseudospin-quintet pairing states in a $J = 3/2$ superconductor that preserves time-reversal symmetry. Within the linear response to a Zeeman field, we calculate the spin susceptibility by using the Green's function that is obtained by solving the Gor'kov equation analytically. The calculated results indicate that the magnetic response of pseudospin-quintet states depends sensitively on the pseudospin structures of the pair potential. The susceptibility tensor in A_{1g} (high symmetry) states is isotropic in real space. For T_{2g} and E_g states, the susceptibility tensor becomes anisotropic in real space. We found in T_{2g} states that the susceptibility tensor has the off-diagonal elements.

Unfortunately, to our knowledge, experimental results of spin susceptibility in $J = 3/2$ superconductors are not available. We believe that the characteristic features such as the large anisotropy and the appearance of off-diagonal elements would be helpful information to confirm $J = 3/2$ superconductivity in experiments.

Acknowledgment The authors are grateful to R. Nomura for useful discussion. This work was supported by JSPS KAKENHI (Nos. JP19K14612, JP20H01857, JP22K03478) and JSPS Core-to-Core Program (No. JPJSCCA20170002). T.S. is supported in part by the establishment of university fellowships towards the creation of science technology innovation from the Ministry of Education, Culture, Sports, Science, and Technology (MEXT) of Japan. S.K. was supported by the CREST project (Grants No. JPMJCR19T2) from Japan Science and Technology Agency (JST).

Appendix A: Normal State

The spin susceptibility in the normal state is give by

$$\chi_N = -\left(\frac{\mu_B}{2}\right)^2 T \sum_{\omega_n} \int \frac{d\boldsymbol{k}}{(2\pi)^d}\, \mathrm{Tr}[G_N(\boldsymbol{k}, i\omega_n)\, \tilde{J}_\mu\, G_N(\boldsymbol{k}, i\omega_n)\, \tilde{J}_\nu], \tag{A·1}$$

$$G_N = \frac{i\omega_n - \xi + \vec{\epsilon}_{\boldsymbol{k}} \cdot \vec{\gamma}}{(i\omega_n - \xi)^2 - \vec{\epsilon}_{\boldsymbol{k}}^{\,2}} = \alpha_N + \beta_N \vec{\epsilon}_{\boldsymbol{k}} \cdot \vec{\gamma},$$

$$\alpha_N = \frac{1}{2}\left[\frac{1}{z_{N+}} + \frac{1}{z_{N-}}\right], \quad \beta_N = \frac{1}{2|\vec{\epsilon}_{\boldsymbol{k}}|}\left[\frac{1}{z_{N+}} - \frac{1}{z_{N-}}\right], \tag{A·2}$$

$$z_{N\pm} = i\omega_n - \xi_\pm, \quad \xi_\pm = \xi \pm |\vec{\epsilon}_{\boldsymbol{k}}|. \tag{A·3}$$

The Green's function is the solution of

$$[i\omega_n - H_N]G_N(\boldsymbol{k}, \omega_n) = 1, \quad H_N(\boldsymbol{k}) = \xi_{\boldsymbol{k}} + \vec{\epsilon}_{\boldsymbol{k}} \cdot \vec{\gamma}. \tag{A·4}$$

The trace of the Green's function is calculated as

$$\mathrm{Tr}[G_N(\boldsymbol{k}, i\omega_n)\, \tilde{J}_\mu\, G_N(\boldsymbol{k}, i\omega_n)\, \tilde{J}_\nu] = \delta_{\mu,\nu}\, P_+ + \alpha_N^2 + \alpha_N\, \beta_N M_{\mu,\nu}(\vec{\epsilon}_{\boldsymbol{k}}) + \beta_N^2 L_{\mu,\nu}(\vec{\epsilon}_{\boldsymbol{k}}), \tag{A·5}$$

where we use $\mathrm{Tr}(\tilde{J}_\mu \tilde{J}_\nu) = P_+\, \delta_{\mu,\nu}$ and define the tensor

$$M_{\mu,\nu}(\vec{\epsilon}) \equiv \mathrm{Tr}[\vec{\epsilon} \cdot \vec{\gamma}(\tilde{J}_\mu\, \tilde{J}_\nu + \tilde{J}_\nu \tilde{J}_\mu)]. \tag{A·6}$$

The angular momenta J_ν are expressed in terms of γ^ν

$$J_x = \frac{-i}{2}\left[\sqrt{3}\gamma^2\gamma^5 + \gamma^1\gamma^3 + \gamma^2\gamma^4\right], \quad J_y = \frac{i}{2}\left[\sqrt{3}\gamma^3\gamma^5 + \gamma^1\gamma^2 - \gamma^3\gamma^4\right], \quad J_z = \frac{i}{2}\left[\gamma^2\gamma^3 + 2\gamma^1\gamma^4\right]. \tag{A·7}$$

They obey the relation $U_T(J^\nu)^* U_T^{-1} = -J^\nu$, which simply means that the angular momenta are antisymmetric under the time-reversal operation. The expression of J_ν^3

$$J_x^3 = -\frac{i}{8}\left(7\sqrt{3}\gamma^2\gamma^5 + 13\gamma^1\gamma^3 + 7\gamma^2\gamma^4\right), \quad J_y^3 = \frac{i}{8}\left(7\sqrt{3}\gamma^3\gamma^5 + 13\gamma^1\gamma^2 - 7\gamma^3\gamma^4\right), \tag{A·8}$$

$$J_z^3 = \frac{i}{8}\left[13\gamma^2\gamma^3 + 14\gamma^1\gamma^4\right], \tag{A·9}$$

suggests that J_ν and J_ν^3 share the common matrix structures. The elements of the tensor are calculated as

$$M_{xx}(\vec{\epsilon}) = 4p_1p_2, \left(\sqrt{3}\epsilon_4 - \epsilon_5\right), \quad M_{yy}(\vec{\epsilon}) = -4p_1p_2, \left(\sqrt{3}\epsilon_4 + \epsilon_5\right), \quad M_{zz}(\vec{\epsilon}) = 8p_1p_2, \epsilon_5, \tag{A·10}$$

$$M_{xy}(\vec{\epsilon}) = M_{yx}(\vec{\epsilon}) = 4\sqrt{3}p_1^2\epsilon_1, \quad M_{xz}(\vec{\epsilon}) = M_{zx}(\vec{\epsilon}) = 4\sqrt{3}p_1^2\epsilon_3, \quad M_{yz}(\vec{\epsilon}) = M_{zy}(\vec{\epsilon}) = 4\sqrt{3}p_1^2\epsilon_2, \tag{A·11}$$

where $\epsilon_j = \beta \boldsymbol{k}^2 e_j c_j(\hat{\boldsymbol{k}})$ as defined in Eq. (4) and we have used the relations

$$\mathrm{Tr}[\gamma^j] = 0, \quad \mathrm{Tr}[\gamma^i\gamma^j] = 4\delta_{i,j}, \quad \mathrm{Tr}[\gamma^i\gamma^j\gamma^k] = 0, \quad \mathrm{Tr}[\gamma^i\gamma^j\gamma^k\gamma^l] = 4[\delta_{i,j}\delta_{k,l} - \delta_{i,k}\delta_{j,l} + \delta_{i,l}\delta_{j,k}]. \tag{A·12}$$

The another tensor $L_{\mu,\nu}$ is defined by Eq. (36).

The summation over the wavenumber is replaced by the integration as

$$\int \frac{d\boldsymbol{k}}{(2\pi)^d} F(\boldsymbol{k}) \to N_0 \int_{-\infty}^{\infty} d\xi \, \langle F(\xi, \hat{\boldsymbol{k}})\rangle_{\hat{\boldsymbol{k}}}, \quad \langle F(\xi, \hat{\boldsymbol{k}})\rangle_{\hat{\boldsymbol{k}}} = \int \frac{d\hat{\boldsymbol{k}}}{4\pi} F(\xi, \hat{\boldsymbol{k}}), \tag{A·13}$$

where $\hat{\boldsymbol{k}}$ is the unit vector on the Fermi surface. By using the relations

$$\langle M_{\mu,\nu}(\vec{\epsilon}_{\boldsymbol{k}})\rangle_{\hat{\boldsymbol{k}}} = 0, \quad \langle L_{\mu,\nu}(\vec{\epsilon}_{\boldsymbol{k}})\rangle_{\hat{\boldsymbol{k}}} = \langle L_{\mu,\mu}\rangle_{\hat{\boldsymbol{k}}}\,\delta_{\mu,\nu}, \tag{A·14}$$

the susceptibility in the normal state becomes

$$\chi_{\mathrm{N}} = -\left(\frac{\mu_{\mathrm{B}}}{2}\right)^2 T\sum_{\omega_n}\int \frac{d\boldsymbol{k}}{(2\pi)^d}\left[P_+\alpha_N^2 + \beta_N^2\langle L_{\mu,\mu}\rangle_{\hat{\boldsymbol{k}}}\right]\delta_{\mu,\nu}. \tag{A·15}$$

The summation over the Matsubara frequency is carried out as

$$T\sum_{\omega_n}\alpha_N^2 = \frac{1}{4}T\sum_{\omega_n}\left[\frac{1}{z_{N+}^2} + \frac{1}{|\vec{\epsilon}_{\boldsymbol{k}}|}\left(\frac{1}{z_{N+}} - \frac{1}{z_{N-}}\right) + \frac{1}{z_{N-}^2}\right], \tag{A·16}$$

$$= \frac{1}{4}\left[-\frac{1}{4T}\cosh^{-2}\frac{\xi_+}{2T} - \frac{1}{2|\vec{\epsilon}_{\boldsymbol{k}}|}\left(\tanh\frac{\xi_+}{2T} - \tanh\frac{\xi_-}{2T}\right) - \frac{1}{4T}\cosh^{-2}\frac{\xi_-}{2T}\right]. \tag{A·17}$$

The integration over ξ after the summation over the frequency can be calculated exactly as

$$\int_{-\infty}^{\infty} d\xi\, T\sum_{\omega_n}\alpha_N^2 = -1, \quad \int_{-\infty}^{\infty} d\xi\, T\sum_{\omega_n}\beta_N^2 = 0. \tag{A·18}$$

The resulting spin susceptibility

$$\chi_{\mathrm{N}} = \left(\frac{\mu_{\mathrm{B}}}{2}\right)^2 P_+ N_0, \tag{A·19}$$

is diagonal and isotropic independent of the direction of a Zeeman field.

The normal Green's function can be described alternatively as

$$G_{\mathrm{N}} = \frac{-1}{Z_N(\omega_n)}\left[A_N + B_N\vec{\epsilon}_{\boldsymbol{k}}\cdot\vec{\gamma}\right], \quad Z_N = \xi^4 + 2\xi^2(\omega_n^2 - \vec{\epsilon}_{\boldsymbol{k}}^{\,2}) + (\omega_n^2 + \vec{\epsilon}_{\boldsymbol{k}}^{\,2})^2 \tag{A·20}$$

$$A_N = (\omega_n^2 + \xi^2 + \vec{\epsilon}_{\boldsymbol{k}}^{\,2})i\omega_n + (\omega_n^2 + \xi^2 - \vec{\epsilon}_{\boldsymbol{k}}^{\,2})\xi, \quad B_N = -\{(i\omega_n - \xi)^2 - \vec{\epsilon}_{\boldsymbol{k}}^{\,2}\}. \tag{A·21}$$

When we carry out the summation over the wavenumber first as

$$N_0\int_{-\infty}^{\infty} d\xi \langle \mathrm{Tr}[G_{\mathrm{N}}(\boldsymbol{k}, i\omega_n)\tilde{J}_\mu G_{\mathrm{N}}(\boldsymbol{k}, i\omega_n)\tilde{J}_\nu]\rangle_{\hat{\boldsymbol{k}}} = N_0\int_{-\infty}^{\infty} d\xi\frac{1}{Z_N^2}\left[\delta_{\mu,\nu}P_+A_N^2 + B_N^2\langle L_{\mu,\nu}\rangle_{\hat{\boldsymbol{k}}}\right], \tag{A·22}$$

we find $\chi_{\mathrm{N}} = 0$ because of

$$\int_{-\infty}^{\infty} d\xi\frac{A_N^2}{Z_N^2} = \int_{-\infty}^{\infty} d\xi\frac{B_N^2}{Z_N^2} = 0. \tag{A·23}$$

The discrepancy is derived from the fact that the integration over the wavenumber and the summation over the frequency do not converge.[29] On the way to Eq. (A·23), we have used the following relations

$$I_0 = \int_{-\infty}^{\infty} d\xi \frac{1}{Z_N} = \frac{\pi}{2|\omega_n|(\omega_n^2+\varepsilon^2)}, \quad J_n = \int_{-\infty}^{\infty} d\xi \frac{\xi^n}{Z_N^2}, \tag{A·24}$$

$$J_0 = \frac{I_0}{8\omega_n^2}\frac{5\omega_n^2+\varepsilon^2}{(\omega_n^2+\varepsilon^2)^2}, \quad J_2 = \frac{I_0}{8\omega_n^2}, \quad J_4 = \frac{I_0}{8\omega_n^2}(\omega_n^2+\varepsilon^2), \quad J_6 = \frac{I_0}{8\omega_n^2}(\omega_n^2+\varepsilon^2)(5\omega_n^2+\varepsilon^2). \tag{A·25}$$

We approximately replace $\vec{\epsilon}_{\hat{k}}^{\,2} > 0$ by $\varepsilon^2 = (\alpha/\beta + 5/4)^{-2}\mu^2$.

Appendix B: Superconducting State

The Green's function under Eq. (32) is calculated to be

$$G(\boldsymbol{k},\omega_n) = \frac{1}{Z_{\rm S}}[A_g + B_g \vec{\epsilon}_{\boldsymbol{k}}\cdot\vec{\gamma}], \tag{B·1}$$

$$A_g = -(\omega_n^2 + \xi_{\boldsymbol{k}}{}^2 + \vec{\eta}_{\boldsymbol{k}}{}^2 + \vec{\epsilon}_{\boldsymbol{k}}{}^2)i\omega_n - (\omega_n^2 + \xi_{\boldsymbol{k}}{}^2 + \vec{\eta}_{\boldsymbol{k}}{}^2 - \vec{\epsilon}_{\boldsymbol{k}}{}^2)\,\xi_{\boldsymbol{k}}, \tag{B·2}$$

$$B_g = \omega_n^2 - \xi^2 - 2i\,\omega_n\,\xi_{\boldsymbol{k}} + \vec{\eta}_{\boldsymbol{k}}{}^2 + \vec{\epsilon}_{\boldsymbol{k}}{}^2, \tag{B·3}$$

$$F(\boldsymbol{k},\omega_n) = \frac{1}{Z_{\rm S}}[A_f + B_f\vec{\eta}_{\boldsymbol{k}}\cdot\vec{\gamma}]U_T, \quad \underset{\sim}{F}(\boldsymbol{k},\omega_n) = \frac{U_T}{Z_{\rm S}}[A_f + B_f\vec{\eta}_{\boldsymbol{k}}\cdot\vec{\gamma}], \tag{B·4}$$

$$A_f = -2\xi_{\boldsymbol{k}}\,\vec{\epsilon}_{\boldsymbol{k}}\cdot\vec{\eta}_{\boldsymbol{k}}, \quad B_f = (\omega_n^2 + \xi_{\boldsymbol{k}}{}^2 + \vec{\eta}_{\boldsymbol{k}}{}^2 + \vec{\epsilon}_{\boldsymbol{k}}{}^2), \tag{B·5}$$

$$Z_{\rm S} = (\omega_n^2 + \xi_{\boldsymbol{k}}{}^2 + \vec{\eta}_{\boldsymbol{k}}{}^2 + \vec{\epsilon}_{\boldsymbol{k}}{}^2)^2 - 4\xi_{\boldsymbol{k}}{}^2\vec{\epsilon}_{\boldsymbol{k}}{}^2 = Z_N(\Omega), \tag{B·6}$$

with $\Omega = \sqrt{\omega_n^2 + \vec{\eta}_{\boldsymbol{k}}{}^2}$. When we carry out the summation over the wavenumber, we find

$$\begin{aligned} N_0 &\int_{-\infty}^{\infty} d\xi \langle {\rm Tr}[G_{\rm S}(\boldsymbol{k},i\omega_n)\,\tilde{J}^{\mu}\,G_{\rm S}(\boldsymbol{k},i\omega_n)\,\tilde{J}^{\nu}]\rangle_{\hat{\boldsymbol{k}}}, \\ &= N_0\int_{-\infty}^{\infty} d\xi \left\langle \left[\left\{ \frac{A_N^2(\Omega)}{Z_N^2(\Omega)} + \frac{\vec{\eta}_{\boldsymbol{k}}{}^2(\Omega^2 + \vec{\epsilon}_{\boldsymbol{k}}{}^2 + \xi^2)^2}{Z_{\rm S}^2}\right\}\tilde{J}_\mu\,\tilde{J}_\nu + \left\{\frac{B_N^2(\Omega)}{Z_N^2(\Omega)} + \frac{4\vec{\epsilon}_{\boldsymbol{k}}{}^2\,\xi^2}{Z_{\rm S}^2}\right\} L_{\mu,\nu}(\vec{\eta}_{\boldsymbol{k}})\right]\right\rangle_{\hat{\boldsymbol{k}}}, \\ &= \left\langle \frac{\pi N_0}{4\Omega^3(\Omega^2+\varepsilon^2)}[P_+\vec{\eta}_{\boldsymbol{k}}{}^2(2\Omega^2+\varepsilon^2)\delta_{\mu,\nu} + \varepsilon^2 L_{\mu,\nu}(\vec{\eta}_{\boldsymbol{k}})]\right\rangle_{\hat{\boldsymbol{k}}}, \end{aligned} \tag{B·7}$$

$$\begin{aligned} N_0 &\int_{-\infty}^{\infty} d\xi \langle {\rm Tr}[\underset{\sim}{F}{\rm S}(\boldsymbol{k},i\omega_n)\,\tilde{J}^{\mu}\,F_{\rm S}(\boldsymbol{k},i\omega_n)(\tilde{J}^{\nu})^*]\rangle_{\hat{\boldsymbol{k}}}, \\ &= N_0\int_{-\infty}^{\infty} d\xi \left\langle \left[\left\{ \frac{4\vec{\eta}_{\boldsymbol{k}}{}^2\,\vec{\epsilon}_{\boldsymbol{k}}{}^2\,\xi^2)}{Z_{\rm S}^2}\right\}\tilde{J}_\mu\,\tilde{J}_\nu + \left\{\frac{(\xi^2+\Omega^2+\vec{\epsilon}_{\boldsymbol{k}}{}^2)^2}{Z_{\rm S}^2}\right\} L_{\mu,\nu}(\vec{\eta}_{\boldsymbol{k}})\right]\right\rangle_{\hat{\boldsymbol{k}}}, \\ &= \left\langle \frac{\pi N_0}{4\Omega^3(\Omega^2+\varepsilon^2)}[P_+\vec{\eta}_{\boldsymbol{k}}{}^2\,\varepsilon^2\delta_{\mu,\nu} + (2\Omega^2+\varepsilon^2)\,L_{\mu,\nu}(\vec{\eta}_{\boldsymbol{k}})]\right\rangle_{\hat{\boldsymbol{k}}}. \end{aligned} \tag{B·8}$$

The average $\langle L_{\mu,\nu}\rangle_{\hat{\boldsymbol{k}}}$ describes the anisotropy and the off-diagonal response of the spin susceptibility.

Appendix C: Gap Equation

The attractive interactions between two electrons are necessary for Cooper pairing. Some bosonic excitation usually mediates the attractive interactions. In this Appendix, we assume the attractive interaction phenomenologically and derive the gap equation for superconducting states discussed in this paper. The pair potential of the superconducting states is defined by

$$\begin{aligned}\Delta_{\alpha,\beta}(\hat{\boldsymbol{k}}) &= \frac{1}{V_{\rm vol}}\sum_{\boldsymbol{k}'}\sum_{\lambda,\tau} V_{\alpha,\beta;\lambda,\gamma}(\boldsymbol{k}-\boldsymbol{k}')\langle c_{\boldsymbol{k}',\lambda}\,c_{-\boldsymbol{k}',\tau}\rangle, \\ &= -\frac{1}{V_{\rm vol}}\sum_{\boldsymbol{k}'} T\sum_{\omega_n}\sum_{\lambda,\tau} V_{\alpha,\beta;\lambda,\tau}(\boldsymbol{k}-\boldsymbol{k}')\,F_{\lambda,\tau}(\boldsymbol{k}',\omega_n),\end{aligned} \tag{C·1}$$

where α, β, λ, and τ are the indices of pseudospin of an electron. The attractive interaction $V_{\alpha,\beta;\lambda,\tau}$ works on two electrons with λ and τ and generates the pair potential between two electrons with α and β. The attractive interaction can be decomposed as

$$V_{\alpha,\beta;\lambda,\tau}(\boldsymbol{k}-\boldsymbol{k}') = \sum_{\nu=1-5} g_\nu(\boldsymbol{k}-\boldsymbol{k}')(\gamma_\nu\,U_T)_{\alpha,\beta}(\gamma_\nu\,U_T)^*_{\lambda,\tau}. \tag{C·2}$$

For A_{1g} states in Sect. 4.1, we choose

$$g_\nu(\boldsymbol{k}-\boldsymbol{k}') = \begin{cases} g\,c_\nu(\hat{\boldsymbol{k}})\,c_\nu(\hat{\boldsymbol{k}}') & \nu = 1\text{–}3 \\ 0 & \nu = 4,5 \end{cases} \quad T_{2g}\ \text{irreps} \tag{C·3}$$

$$g_\nu(\boldsymbol{k}-\boldsymbol{k}') = \begin{cases} 0 & \nu = 1\text{–}3 \\ g\,c_\nu(\hat{\boldsymbol{k}})\,c_\nu(\hat{\boldsymbol{k}}') & \nu = 4,5 \end{cases} \quad E_g\ \text{irreps} \tag{C·4}$$

$$g_\nu(\boldsymbol{k}-\boldsymbol{k}') = g\,c_\nu(\hat{\boldsymbol{k}})\,c_\nu(\hat{\boldsymbol{k}}'), \quad \nu = 1\text{–}5 \quad T_{2g}+E_g\ \text{irreps}. \tag{C·5}$$

By substituting the anomalous Green's function in Eq. (B·4) into Eq. (C·1), we obtain the gap equation

$$\Delta = T\sum_{\omega_n} gN_0\int d\xi\,\frac{B_f\,\Delta}{Z_{\rm S}}, \tag{C·6}$$

where we have used Eq. (8). After integrating over ξ, we obtain

$$1 = gN_0T\sum_{\omega_n}\frac{1}{\sqrt{\omega_n^2+\Delta^2}}. \tag{C·7}$$

The results coinsides with the gap equation in BCS theory. For T_{2g}, E_g, and an admixture state of them in Sects. 4.2 and 4.3, we replace $c_\nu(\hat{\boldsymbol{k}})$ by 1 for all ν in Eqs. (C·3)–(C·5). The gap equation for such states is identical to Eq. (C·7).

1) C. Fang, H. Weng, X. Dai, and Z. Fang, Chin. Phys. B **25**, 117106 (2016).
2) N. P. Armitage, E. J. Mele, and A. Vishwanath, Rev. Mod. Phys. **90**, 015001 (2018).
3) M. Z. Hasan and C. L. Kane, Rev. Mod. Phys. **82**, 3045 (2010).
4) X.-L. Qi and S.-C. Zhang, Rev. Mod. Phys. **83**, 1057 (2011).
5) Y. Tanaka, M. Sato, and N. Nagaosa, J. Phys. Soc. Jpn. **81**, 011013 (2012).
6) M. Sato and S. Fujimoto, J. Phys. Soc. Jpn. **85**, 072001 (2016).
7) T. Mizushima, Y. Tsutsumi, T. Kawakami, M. Sato, M. Ichioka, and K. Machida, J. Phys. Soc. Jpn. **85**, 022001 (2016).
8) C.-K. Chiu, J. C. Y. Teo, A. P. Schnyder, and S. Ryu, Rev. Mod. Phys. **88**, 035005 (2016).
9) M. Sato and Y. Ando, Rep. Prog. Phys. **80**, 076501 (2017).
10) N. P. Butch, P. Syers, K. Kirshenbaum, A. P. Hope, and J. Paglione, Phys. Rev. B **84**, 220504 (2011).
11) Y. Nakajima, R. Hu, K. Kirshenbaum, A. Hughes, P. Syers, X. Wang, K. Wang, R. Wang, S. R. Saha, D. Pratt, J. W. Lynn, and J. Paglione, Sci. Adv. **1**, e1500242 (2015).
12) P. M. R. Brydon, L. Wang, M. Weinert, and D. F. Agterberg, Phys. Rev. Lett. **116**, 177001 (2016).
13) D. F. Agterberg, P. M. R. Brydon, and C. Timm, Phys. Rev. Lett. **118**, 127001 (2017).
14) S. Kobayashi, A. Bhattacharya, C. Timm, and P. M. R. Brydon, Phys. Rev. B **105**, 134507 (2022).
15) P. M. R. Brydon, D. F. Agterberg, H. Menke, and C. Timm, Phys. Rev. B **98**, 224509 (2018).
16) H. Kim, K. Wang, Y. Nakajima, R. Hu, S. Ziemak, P. Syers, L. Wang, H. Hodovanets, J. D. Denlinger, P. M. R. Brydon, D. F. Agterberg, M. A. Tanatar, R. Prozorov, and J. Paglione, Sci. Adv. **4**, eaao4513 (2018).
17) J. W. F. Venderbos, L. Savary, J. Ruhman, P. A. Lee, and L. Fu, Phys. Rev. X **8**, 011029 (2018).
18) S. Kobayashi, A. Yamakage, Y. Tanaka, and M. Sato, Phys. Rev. Lett. **123**, 097002 (2019).
19) D. Kim, S. Kobayashi, and Y. Asano, Phys. Rev. B **103**, 184516 (2021).
20) D. Kim, S. Kobayashi, and Y. Asano, J. Phys. Soc. Jpn. **90**, 104708 (2021).
21) Y. Xiong, A. Yamakage, S. Kobayashi, M. Sato, and Y. Tanaka, Crystals **7**, 58 (2017).
22) Y. Yamazaki, S. Kobayashi, and A. Yamakage, J. Phys. Soc. Jpn. **90**, 073701 (2021).
23) S. Kobayashi, Y. Yamazaki, A. Yamakage, and M. Sato, Phys. Rev. B **103**, 224504 (2021).
24) K. Yosida, Phys. Rev. **110**, 769 (1958).
25) J. Yu and C.-X. Liu, J. Appl. Phys. **128**, 063904 (2020).
26) G. D. Mahan, *Many-Particle Physics* (Plenum, New York, 1990).
27) J. M. Luttinger and W. Kohn, Phys. Rev. **97**, 869 (1955).
28) D. Zhang, H. Wang, J. Ruan, G. Yao, and H. Zhang, Phys. Rev. B **97**, 195139 (2018).
29) A. A. Abrikosov, L. P. Gor'kov, and I. E. Dzyaloshinski, *Methods of Quantum Field Theory in Statistical Physics* (Dover, New York, 1975).
30) M. Sigrist and K. Ueda, Rev. Mod. Phys. **63**, 239 (1991).
31) Y. Asano and A. Sasaki, Phys. Rev. B **92**, 224508 (2015).
32) Y. Tanaka, Y. Asano, A. A. Golubov, and S. Kashiwaya, Phys. Rev. B **72**, 140503 (2005).
33) Y. Asano, A. A. Golubov, Y. V. Fominov, and Y. Tanaka, Phys. Rev. Lett. **107**, 087001 (2011).
34) S.-I. Suzuki and Y. Asano, Phys. Rev. B **89**, 184508 (2014).
35) S.-I. Suzuki, T. Sato, and Y. Asano, Phys. Rev. B **106**, 104518 (2022).
36) P. A. Frigeri, D. F. Agterberg, and M. Sigrist, New J. Phys. **6**, 115 (2004).
37) H. Menke, C. Timm, and P. M. R. Brydon, Phys. Rev. B **100**, 224505 (2019).
38) A. Ramires, D. F. Agterberg, and M. Sigrist, Phys. Rev. B **98**, 024501 (2018).